Available online at www.sciencedirect.com
ScienceDirect
Physica A 375 (2007) 247–256
PHYSICA A
www.elsevier.com/locate/physa

Two-lane totally asymmetric exclusion processes with particle creation and annihilation

Rui Jiang[a,*], Ruili Wang[b], Qing-Song Wu[a]

[a]School of Engineering Science, University of Science and Technology of China, Hefei 230026, China
[b]Institute of Information Sciences and Technology, Massey University, New Zealand

Received 11 May 2006; received in revised form 9 August 2006
Available online 7 September 2006

Abstract

This paper studies two-lane totally asymmetric simple exclusion processes (TASEP) coupled with particle creation and annihilation in one of the two lanes (lane 2). The dependence of the density profiles of both lanes on the lane-change rate Ω is investigated. It is shown that with the increase of Ω, a complex behavior on both lanes occurs. Synchronization of the shocks in both lanes occurs when Ω exceeds a threshold $\Omega_c \approx 10$. A boundary layer is also observed at the left boundary as a finite-size effect. The situations arising from very large creation/annihilation rate and very small creation/annihilation rate are also investigated. The mean-field analysis is presented and it agrees well with Monte Carlo simulations.

Keywords: ASEP; Langmuir kinetics; Two-lane

1. Introduction

In recent years, asymmetric simple exclusion processes (ASEPs) have become an important tool for investigation of many processes in chemistry, physics and biology [1,2]. ASEPs were introduced in 1968 as theoretical models for describing the kinetics of biopolymerization [3] and have been applied successfully to understand polymer dynamics in dense media [4], diffusion through membrane channels [5], gel electrophoresis [6], dynamics of motor proteins moving along rigid filaments [7], the kinetics of synthesis of proteins [8], and traffic flow analysis [9,10].

ASEPs are discrete non-equilibrium models that describe the stochastic dynamics of multi-particle transport along one-dimensional lattices. Each lattice site can be either empty or occupied by a single particle. Particles interact only through hard core exclusion potential. Exact solutions for the stationary state exist for periodic [11] and open boundary conditions [12] and different update schemes [13–15]. The simplest limit of ASEP is that particles can only move in one direction. This is called the totally asymmetric simple exclusion process (TASEP).

*Corresponding author.
E-mail address: rjiang@ustc.edu.cn (R. Jiang).

0378-4371/$ - see front matter © 2006 Elsevier B.V. All rights reserved.
doi:10.1016/j.physa.2006.08.025

Recently, the coupling of ASEPs with different equilibrium and non-equilibrium processes has led to many unusual and unexpected phenomena. For example, Popkov et al. considered parallel-chain ASEPs [16–18]. However, in these investigations the coupling between different chains was indirect, i.e., hopping between the chains was forbidden. Pronina and Kolomeisky studied two-chain asymmetric exclusion processes, in which particles can move between the lattice channels [19]. Mitsudo and Hayakawa extended the two-lane model [19] to a case incorporating the asymmetric lane-change rule and boundary parameters and found the synchronization of kinks [20]. Parmeggiani et al. investigated the interplay of TASEP with the creation and annihilation of particles (Langmuir kinetics, LK) [21]. The phenomenon of localized density shocks was produced and was explained by applying a phenomenological domain wall theory [22–25].

The aim of the present paper is to investigate the coupling of two-lane TASEP with LK and to study the shocks in both lanes. This is relevant for studies of, e.g., motor proteins kinetics moving along the parallel protofilaments of microtubules without restrictions for them to jump between these protofilaments and of two-lane traffic models with bulk on–off ramps (such as parking places along the road). This paper discusses the case where creation and annihilation of particles occur only in one of the two lanes. A mean-field analysis is presented and computer Monte Carlo (MC) simulations are performed to validate our mean-field analysis.

The paper is organized as follows. In Section 2 we give a description of the two-lane TASEP model, considering the creation and annihilation of particles. In Section 3, we present and discuss the results of MC simulations. In Section 4, a mean-field analysis is presented and is shown to agree well with MC simulation results. Finally, we give our conclusions in Section 5.

2. Model

Our model is defined in a two-lane lattice of $N \times 2$ sites, where N is the length of a lane. We introduce an occupation variable $\tau_{\ell,i}$ where $\tau_{\ell,i} = 1$ (or $\tau_{\ell,i} = 0$) indicates that the state of the ith site in the ℓth lane is occupied (or vacant). We apply the following dynamical rules (also see Fig. 1). For each time step, a site (ℓ, i) is chosen at random.

- Case $\ell = 1$ (i.e., lane 1):
  - Subcase $i = 1$: (i) If $\tau_{1,1} = 0$, a particle enters the system with probability α. (ii) If $\tau_{1,1} = 1$ and $\tau_{1,2} = 0$, then the particle in the site of $(1, 1)$ moves into site $(1, 2)$. (iii) If $\tau_{1,1} = 1$ and $\tau_{1,2} = 1$, then the particle in the site of $(1, 1)$ stays there. No lane change occurs here [27].
  - Subcase $i = N$. If $\tau_{1,N} = 1$, the particle leaves the system with probability β. No lane change occurs [28].
  - Subcase $1 < i < N$. If $\tau_{1,i} = 1$, the particle moves into site $(1, i + 1)$ if $\tau_{1,i+1} = 0$. Otherwise, it changes to lane 2 with probability ω if $\tau_{2,i} = 0$.
- Case $\ell = 2$ (i.e., lane 2):
  - Subcase $i = 1$. (i) If $\tau_{2,1} = 0$, a particle enters the system with probability α. (ii) If $\tau_{2,1} = 1$ and $\tau_{2,2} = 0$, then the particle in the site of $(2, 1)$ moves into site $(2, 2)$. (iii) If $\tau_{2,1} = 1$ and $\tau_{2,2} = 1$, then the particle in

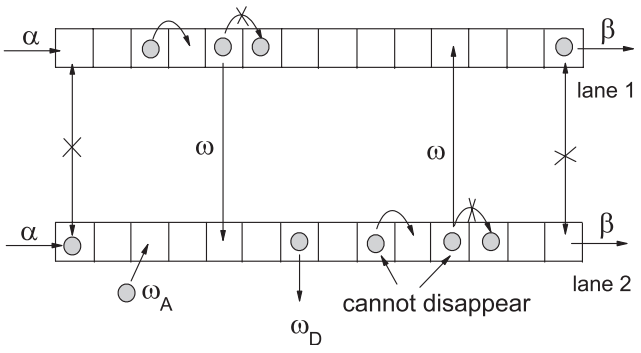

Fig. 1. Two-lane TASEP scheme with bulk creation/annihilation in one of the two lanes (i.e., lane 2).

the site of $(2, 1)$ stay there. No lane change occurs. In other words, all situations in this subcase are similar to that in lane 1.

- Subcase $i = N$. If $\tau_{2,N} = 1$, the particle leaves the system with probability β. This is also similar to the situation in lane 1.
- Subcase $1 < i < N$. (i) If $\tau_{2,i} = 1$, the particle may leave the system with probability ω_D. If it cannot leave the system, then it moves into site $(2, i + 1)$ if $\tau_{2,i+1} = 0$. Otherwise, it changes to lane 1 with probability ω if $\tau_{1,i} = 0$. (ii) If $\tau_{2,i} = 0$, a particle enters the system with probability ω_A.

3. Simulation results

In this section, the results of MC simulations are presented. For the problem of a single-lane ASEP with creation and annihilation, if the rates of creation/annihilation scale correctly with the system length, one observes a subtle interplay between the left and right particle reservoirs. Therefore, as in Ref. [21], we define the lane-exchange rate Ω as $\Omega = \omega N$. For the deduced rates Ω_A and Ω_D [23], they are defined as $\Omega_A = \omega_A N$ and $\Omega_D = \omega_D N$. Also, $K = \Omega_A/\Omega_D$.

Figs. 2 and 3 show the density profiles of both lanes for various values of Ω. The parameters are set to $N = 1000$, $\alpha = 0.2$, $\beta = 0.6$, $\Omega_D = 0.2$ and $K = 3$. In simulations, stationary profiles are obtained over 10^5 time averages (with a typical time interval of $10\,N$ between each average step). The first $10^5\,N$ time steps are discarded to let the transient time out. For the special case of $\Omega = 0$ (see Fig. 2(a)), the two-lane process retreats to two separated processes: an ASEP (lane 1) and an ASEP with creation and annihilation (lane 2). Therefore, for the given parameters, the density remains constant in lane 1 (except near the right boundary) and a shock appears in lane 2.

When $\Omega > 0$, particles can change lane. With the increase of Ω, the location of the shock in lane 2 shifts right (see Fig. 2). Also, both the amplitude and density of the shock decrease. At the same time, the slope of the bulk density in lane 1 increases [29].

When Ω further increases, the shock begins to appear in lane 1 at $x = x_1$ (see Fig. 3(a) where $\Omega = 0.65$) [30]. We denote the location of the shock in lane 2 as $x = x_2$. It can be seen that the density in lane 2 is divided into the following three ranges: (i) In the range of $x < x_2$, the density increases with x (the slope is denoted as s_1). (ii) In the range of $x_2 < x < x_1$, the density also increases with x but the slope s_2 is different from s_1. (iii) For $x > x_1$, the density decreases with x.

As Ω increases, the shock in lane 2 moves further right first, but its amplitude decreases (see Fig. 3(a) where $\Omega = 0.65$, also see Fig. 3(b) where $\Omega = 1.0$). The slope s_2 increases. The shock in lane 1 moves left and its

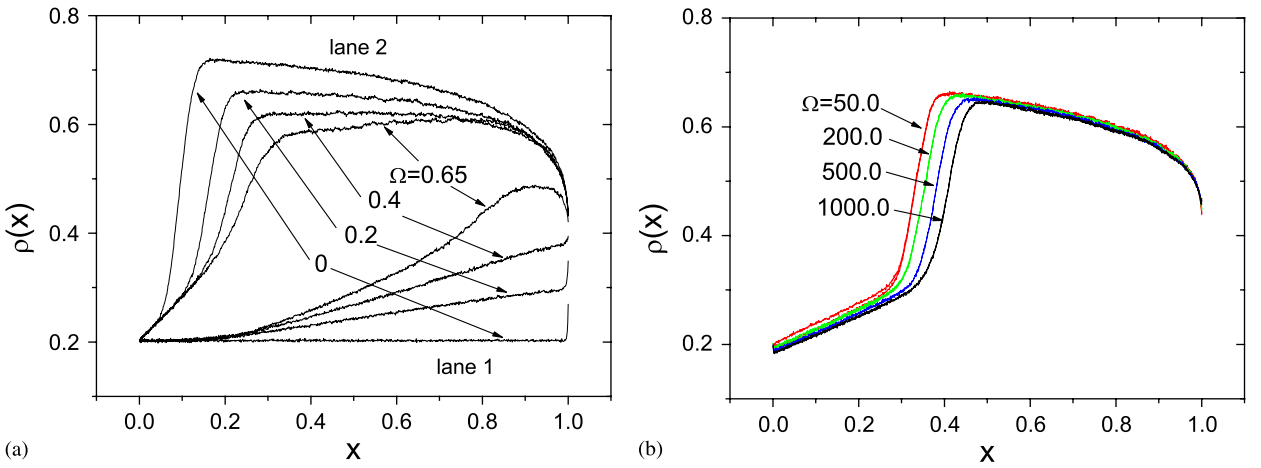

Fig. 2. (Color online) Density profiles from MC simulations for different values of Ω. In (b), the density profiles of the two lanes are synchronized. The system size $N = 1000$, $\Omega_A = 0.6$, $\Omega_D = 0.2$, $\alpha = 0.2$, $\beta = 0.6$.

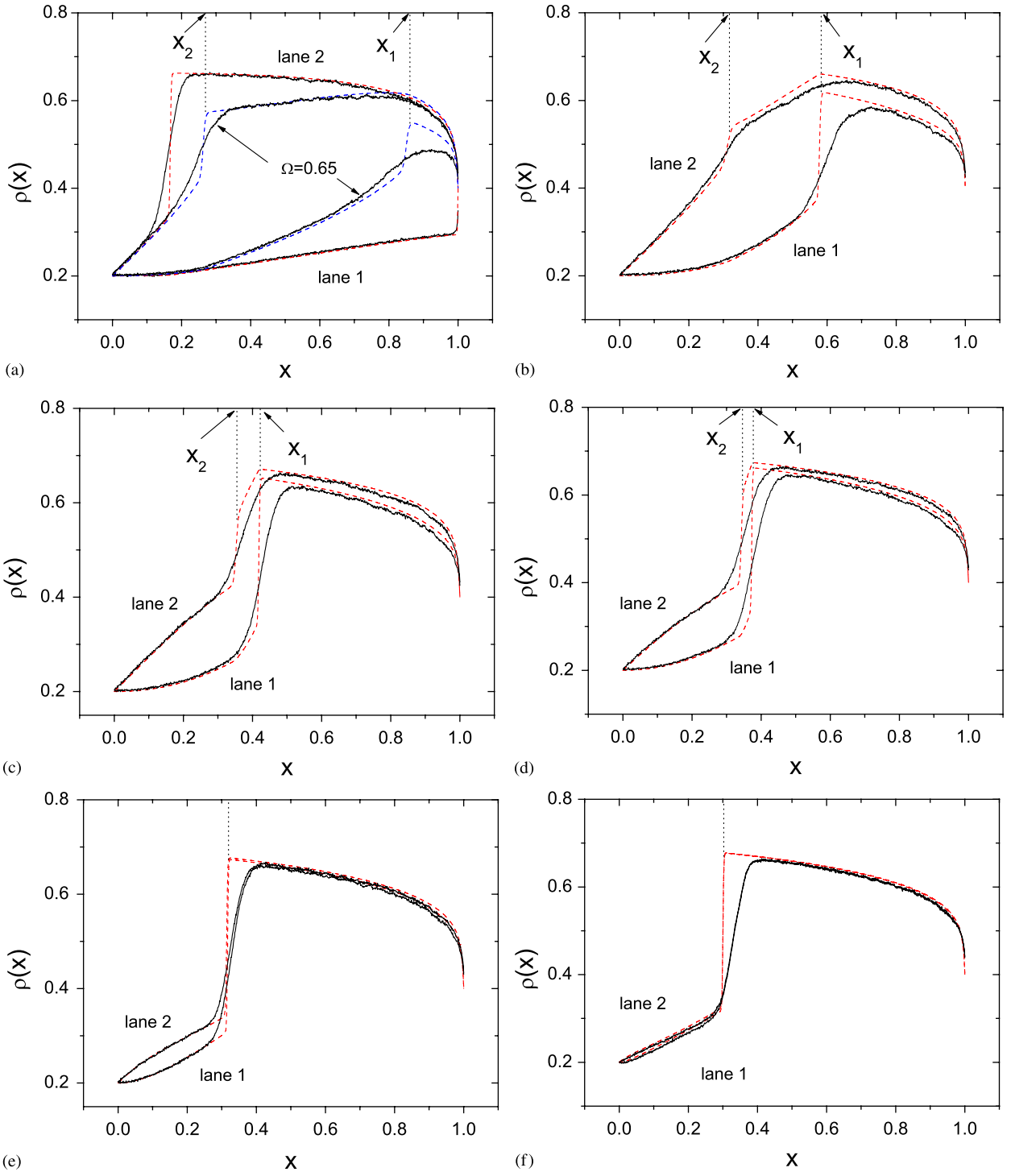

Fig. 3. (Color online) Comparison of the results of a mean-field analysis (dashed) with the results of MC simulations (solid). The parameters are $\Delta t' = 0.001$, $\Delta x = 0.002$, $N = 1000$, $\Omega_A = 0.6$, $\Omega_D = 0.2$, $\alpha = 0.2$, $\beta = 0.6$. (a) $\Omega = 0.2$ and $\Omega = 0.65$, (b) $\Omega = 1.0$, (c) $\Omega = 2.0$, (d) $\Omega = 3.0$, (e) $\Omega = 10.0$, (f) $\Omega = 50.0$.

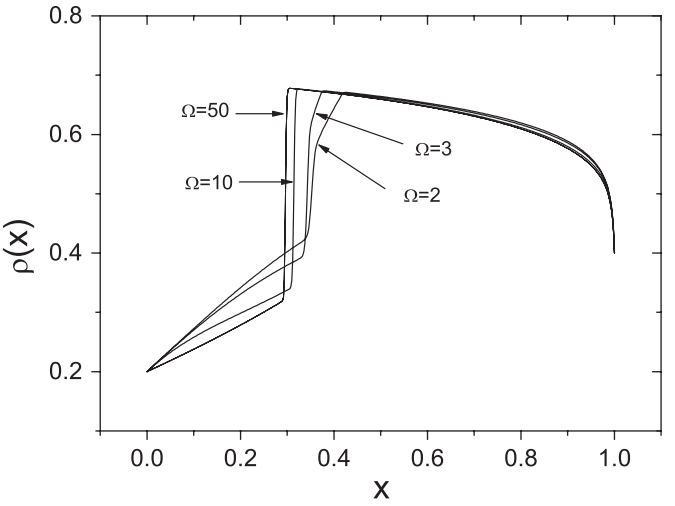

Fig. 4. Density profiles in lane 2 for different values of Ω. The results are from mean-field analysis. The parameters are $\Delta t' = 0.001$, $\Delta x = 0.002$, $N = 1000$, $\Omega_A = 0.6$, $\Omega_D = 0.2$, $\alpha = 0.2$, $\beta = 0.6$.

amplitude increases. Details are as follows:

- When Ω increases from 1.0 to 2.0, the shock in lane 2 still moves right, the slope s_2 still increases, but its amplitude increases (see Figs. 3(b) and (c)). The shock in lane 1 moves left and its amplitude increases.
- When Ω increases from 2.0 to 3.0, the shock in lane 2 moves left slightly (see Fig. 4), both the slope s_2 and its amplitude increase (see Figs. 3(c) and (d)). The shock in lane 1 moves left and its amplitude increases.
- When Ω increases from 3.0 to 10.0, one finds the shock in lane 2 moves left (see Fig. 4), its amplitude increases (see Figs. 3(d) and (e)). The shock in lane 1 moves left and its amplitude increases. For $\Omega = 10$, the shocks in both lanes become synchronized.
- When Ω increases from 10.0 to 50.0, the synchronized shocks move left (see Figs. 3(e) and (f)).

When $\Omega > 50.0$, the synchronized shocks move right as Ω increases. Furthermore, the density profile near the left boundary begins to decrease, i.e., a boundary layer is appearing at $x = 0$ (Fig. 2(b)).

This is explained as follows. When Ω is large, the particles can change lane easily when they are hindered. As a result, the probability that a particle at $i = 1$ is hindered by another particle at $i = 2$ which comes from the other lane increases, which means the "real density" on site $i = 2$ is higher than the "calculated density". Therefore, the actual flow rate from $i = 1$ to 2 decreases due to the higher "real density" on site $i = 2$. Consequently, the boundary layer forms.

However, with the increase of system size, the boundary layer weakens (Fig. 5). Therefore, we believe the boundary layer is a finite-size effect and in the limit of infinite system, the boundary layer will disappear.

Next we investigate the bulk density profile, i.e., the profile of $(\rho_1 + \rho_2)/2$. The results are shown in Fig. 6. This shows that as Ω increases, the density decreases on the left side of the bulk and increases on the right side of the bulk. Finally, a stronger shock can be observed when $\Omega > 1.5$.

We have changed the parameters and found out that provided there is a shock in lane 2 in the case of $\Omega = 0$, the results are similar to those presented above when Ω increases.

However, if Ω_A and Ω_D are so large that the creation and annihilation dominate lane 2 in the case of $\Omega = 0$, different results appear. In Fig. 7, we show the results at different values of Ω, where $\Omega_D = 10$ and $K = 3$. It can be seen that the density profile in lane 2 is independent of Ω. However, as Ω increases, a shock appears in lane 1, then it moves left and its amplitude increases. Finally the density profile in lane 1 becomes identical to that in lane 2.

This is interpreted as follows. Here lane 2 acts as a homogeneous bulk reservoir for lane 1. The problem, therefore, reduces to a single lane TASEP with creation and annihilation of particles. The difference from the TASEP coupled with LK comes from the fact that the creation and annihilation rules are different.

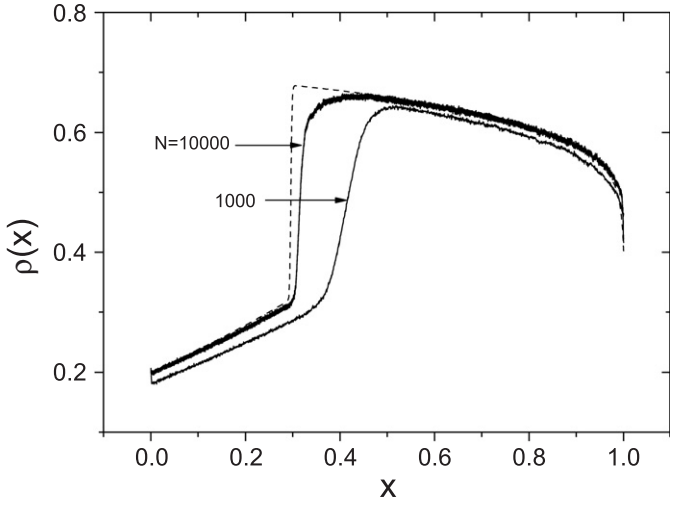

Fig. 5. Density profile where $\Omega = 1000$. The dashed line is the result from mean-field analysis. The parameters are $\Delta t' = 0.001$, $\Delta x = 0.002$, $\Omega_A = 0.6$, $\Omega_D = 0.2$, $\alpha = 0.2$, $\beta = 0.6$.

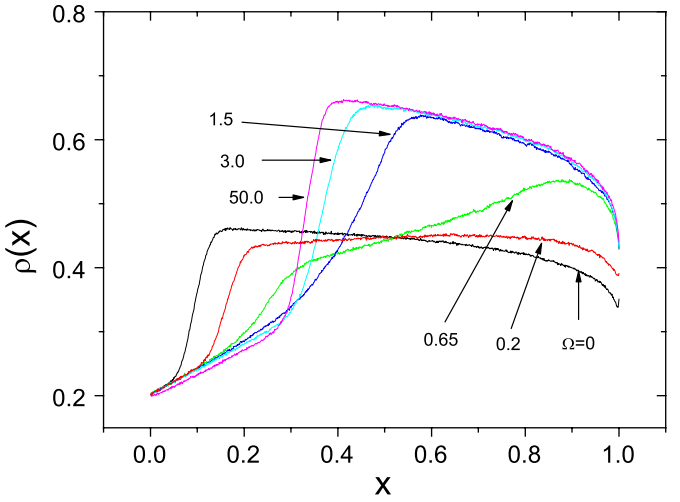

Fig. 6. (Color online) Bulk density profiles for different values of Ω. The parameters are $N = 1000$, $\Omega_A = 0.6$, $\Omega_D = 0.2$, $\alpha = 0.2$, $\beta = 0.6$.

The annihilation is fulfilled by changing to lane 2 and the creation is fulfilled by changing lane from lane 2. Therefore, increasing lane changing rate Ω in this problem is just like increasing Ω_A and Ω_D in TASEP coupled with LK. As a result, the shock forms on lane 1 when Ω increases (c.f. Fig. 2 in Ref. [21]).

When Ω_A and Ω_D are very small, no shock will appear on both lanes. In Fig. 8, we show the density profiles with different values of Ω, where $\Omega_D = 0.002$ and $K = 3$. It can be seen that as Ω increases, the density of the whole system decreases and a boundary layer forms at $x = 0$ similar to Fig. 2(b).

4. Mean-field analysis

In this section, a mean-field theory is developed. The exact equation for the evolution of particle densities $\langle \tau_{\ell,i} \rangle$ excluding the boundaries (i.e., $1 < i < N$) is given by

$$\frac{\mathrm{d}\langle \tau_{1,i} \rangle}{\mathrm{d}t} = \langle \tau_{1,i-1}(1-\tau_{1,i}) \rangle - \langle \tau_{1,i}(1-\tau_{1,i+1}) \rangle + \omega \langle \tau_{2,i}\tau_{2,i+1}(1-\tau_{1,i}) \rangle - \omega \langle \tau_{1,i}\tau_{1,i+1}(1-\tau_{2,i}) \rangle, \quad (1)$$

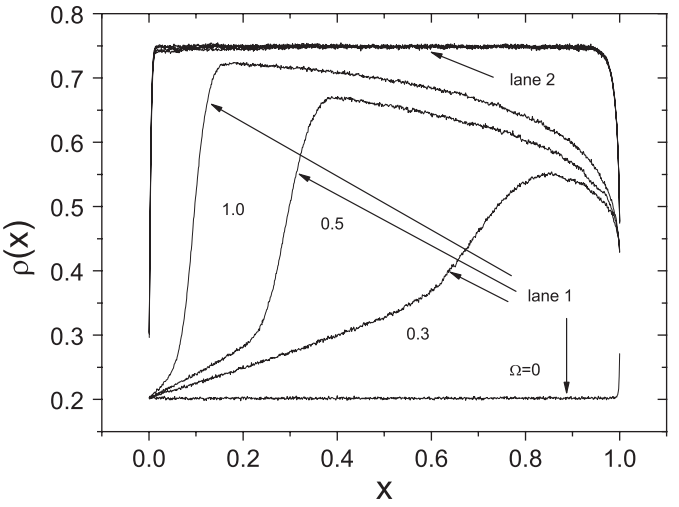

Fig. 7. Density profiles from MC simulations for different values of Ω. The parameters are $N = 1000$, $\Omega_A = 30$, $\Omega_D = 10$, $\alpha = 0.2$, $\beta = 0.6$.

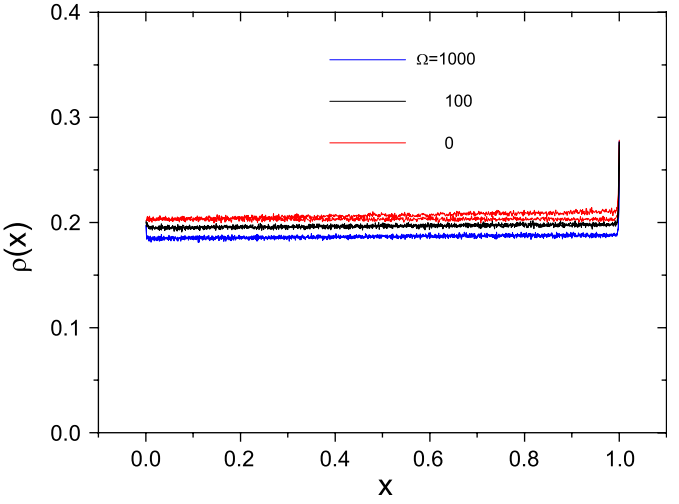

Fig. 8. (Color online) Density profiles from MC simulations for different values of Ω. The parameters are $N = 1000$, $\Omega_A = 0.006$, $\Omega_D = 0.002$, $\alpha = 0.2$, $\beta = 0.6$. The slightly higher density profile in red corresponds to lane 2. For $\Omega = 100$ and 1000, the density profiles in both lanes are identical.

$$\frac{d\langle\tau_{2,i}\rangle}{dt} = \langle\tau_{2,i-1}(1-\tau_{2,i})\rangle - \langle\tau_{2,i}(1-\tau_{2,i+1})\rangle + \omega_A\langle 1-\tau_{2,i}\rangle - \omega_D\langle\tau_{2,i}\rangle + \omega\langle\tau_{1,i}\tau_{1,i+1}(1-\tau_{2,i})\rangle - \omega\langle\tau_{2,i}\tau_{2,i+1}(1-\tau_{1,i})\rangle, \quad (2)$$

where $\langle\cdots\rangle$ denotes a statistical average. Here the term $\omega\langle\tau_{1,i}\tau_{1,i+1}(1-\tau_{2,i})\rangle$ is the average current from site i in lane 1 to site i in lane 2, while $\omega\langle\tau_{2,i}\tau_{2,i+1}(1-\tau_{1,i})\rangle$ is the average current from site i in lane 2 to site i in lane 1. At the boundaries, the densities evolve as

$$\frac{d\langle\tau_{\ell,1}\rangle}{dt} = -\langle\tau_{\ell,1}(1-\tau_{\ell,2})\rangle + \alpha\langle 1-\tau_{\ell,1}\rangle, \quad (3)$$

$$\frac{d\langle\tau_{\ell,N}\rangle}{dt} = \langle\tau_{\ell,N-1}(1-\tau_{\ell,N})\rangle - \beta\langle\tau_{\ell,N}\rangle. \quad (4)$$

When N is large, we can make the continuum mean-field approximation to Eqs. (1) and (2). First, we factorize correlation functions by replacing $\langle\tau_{\ell,i}\rangle$ and $\langle\tau_{\ell,i+1}\rangle$ with $\rho_{\ell,i}$ and $\rho_{\ell,i+1}$, then we set

$$\rho_{\ell,i\pm1} = \rho(x) \pm \frac{1}{N}\frac{\partial\rho}{\partial x} + \frac{1}{2N^2}\frac{\partial^2\rho}{\partial x^2}\cdots. \tag{5}$$

Substituting (5) into Eqs. (1) and (2), we obtain [31]

$$\frac{\partial\rho_1}{\partial t'} = \frac{1}{2N}\frac{\partial^2\rho_1}{\partial x^2} + (2\rho_1 - 1)\frac{\partial\rho_1}{\partial x} + \Omega(1-\rho_1)\rho_2^2 - \Omega\rho_1^2(1-\rho_2), \tag{6}$$

$$\frac{\partial\rho_2}{\partial t'} = \frac{1}{2N}\frac{\partial^2\rho_2}{\partial x^2} + (2\rho_2 - 1)\frac{\partial\rho_2}{\partial x} + \Omega_A(1-\rho_2) - \Omega_D\rho_2 - \Omega(1-\rho_1)\rho_2^2 + \Omega\rho_1^2(1-\rho_2), \tag{7}$$

where $t' = t/N$, $\Omega = \omega N$ and $\Omega_{A,D} = \omega_{A,D}N$. The boundary conditions become $\rho_\ell(x=0) = \alpha$ and $\rho_\ell(x=1) = (1-\beta)$.

The density profiles of the two lanes can be calculated by setting the time derivatives of Eqs. (6) and (7) to zero. As it is difficult to obtain analytical solutions, we analyze the mean-field equations numerically. We discretize Eqs. (6) and (7) into

$$\begin{aligned}\frac{\rho_{1,i}^{n+1} - \rho_{1,i}^n}{\Delta t'} = {} & \frac{1}{2N}\frac{\rho_{1,i-1}^n - 2\rho_{1,i}^n + \rho_{1,i+1}^n}{\Delta x^2} + (2\rho_{1,i}^n - 1)\frac{\rho_{1,i+1}^n - \rho_{1,i-1}^n}{2\Delta x} \\ & + \Omega(1-\rho_{1,i}^n)(\rho_{2,i}^n)^2 - \Omega(\rho_{1,i}^n)^2(1-\rho_{2,i}^n),\end{aligned} \tag{8}$$

$$\begin{aligned}\frac{\rho_{2,i}^{n+1} - \rho_{2,i}^n}{\Delta t'} = {} & \frac{1}{2N}\frac{\rho_{2,i-1}^n - 2\rho_{2,i}^n + \rho_{2,i+1}^n}{\Delta x^2} + (2\rho_{2,i}^n - 1)\frac{\rho_{2,i+1}^n - \rho_{2,i-1}^n}{2\Delta x} \\ & - \Omega(1-\rho_{1,i}^n)(\rho_{2,i}^n)^2 + \Omega(\rho_{1,i}^n)^2(1-\rho_{2,i}^n) \\ & + \Omega_A(1-\rho_{2,i}^n) - \Omega_D\rho_{2,i}^n,\end{aligned} \tag{9}$$

where n is the time-step index, and $\Delta t'$ and Δx are the time step and the space step, respectively. We assume that the density profile at $n = 0$ is homogeneous $\rho_{1,2}(x) = \rho_0$ $(0 < x < 1)$. The density profiles at steady state can be obtained from Eqs. (8) and (9) when $n \to \infty$.

Fig. 9 shows the results of the mean-field analysis. It can been seen that as $n \to \infty$, the density profiles approach those of a steady state and the steady state profile is independent of the density profile at $n = 0$.

In Fig. 3, we compare the results of the mean-field analysis with the results of MC simulations. We find good agreement between the results of the mean-field analysis and the results of MC simulations, which validates our mean-field analysis.

However, in the finite size, when Ω is large, the deviation from the MC simulation results is obvious (Fig. 5), especially at the left bulk, where the boundary layer exists. This is, as we mentioned before, maybe due to a finite-size effect. With the increase of system size, the deviation shrinks.

5. Conclusion

In this paper, the density profiles of TASEPs coupled with particle creation and annihilation in one of the two lanes are investigated with mean-field analysis and using computer MC simulations. The mean-field analysis results agree well with the results of MC simulations. It is found that as Ω increases, a complex behavior on two lanes occur:

- With the increase of Ω, the amplitude of the shock in lane 2 first decreases and then increases. It first moves right and then moves left slightly.
- A shock appears in lane 1 when $\Omega \gtrsim 0.6$ and its amplitude increases as Ω increases. It moves left. The synchronization of the shocks of the two lanes occurs when $\Omega \gtrsim 10.0$.
- When Ω is large, the synchronized shock moves right and a boundary layer appears at $x = 0$. We believe the boundary layer is due to a finite-size effect.

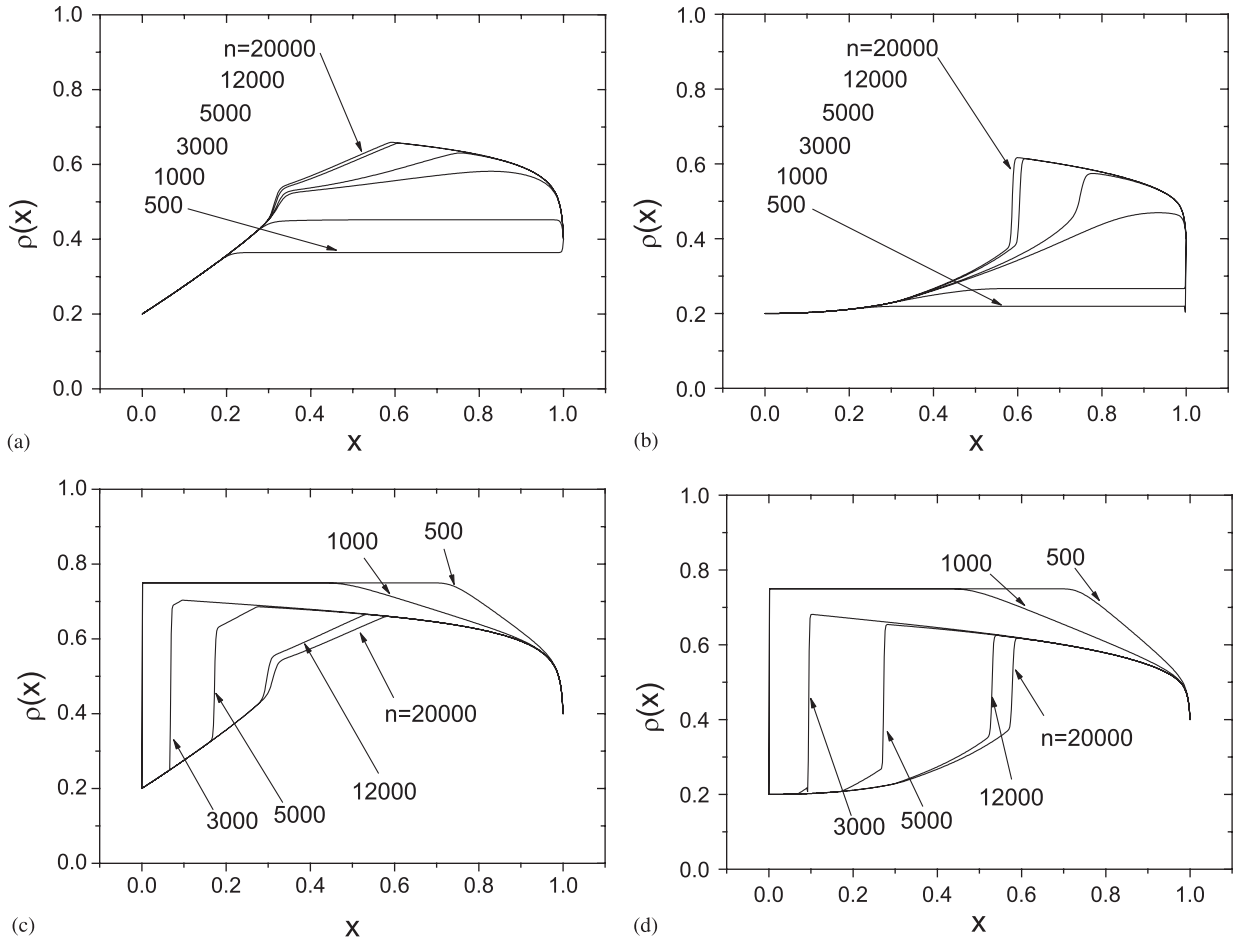

Fig. 9. Evolution of the density profile from a homogeneous one at $n = 0$ according to Eqs. (8) and (9). (a) and (b) start from $\rho_0 = 0.2$; (c) and (d) start from $\rho_0 = 0.75$. (a) and (c) are the density profiles of lane 2; (b) and (d) are the density profile of lane 1. The parameters are $\Delta t' = 0.001$, $\Delta x = 0.002$, $N = 1000$, $\Omega = 1.0$, $\Omega_A = 0.6$, $\Omega_D = 0.2$, $\alpha = 0.2$ and $\beta = 0.6$. When $n > 20\,000$, the profile is almost unchanged. It can be seen that the steady state density profile is the same in (a) and (c), also in (b) and (d).

The situations arising from very large Ω_A (Ω_D) and very small Ω_A (Ω_D) are also investigated and different results are found.

There are several extensions of the model, which can be explored in the future. For example, an asymmetric lane-change rule can be used as in Ref. [20]. We can also consider the situation in which the creation and annihilation occur in both lanes, or the creation occurs in one lane while annihilation in the other. Finally, the situation that there are two or more species of particles in a system would be much more complex and interesting [26].

Acknowledgments

We acknowledge the support of National Basic Research Program of China (2006CB705500), the National Natural Science Foundation of China (NNSFC) under Key Project No. 10532060 and Project Nos. 10404025, 70501004, the CAS special funding, the Open Project of Key Laboratory of Intelligent Technologies and Systems for Traffic and Transportation, Ministry of Education, Beijing Jiaotong University. R. Wang acknowledges the support of the ASIA:NZ Foundation Higher Education Exchange Program (2005) and Massey Research Fund (2005).

References

[1] B. Derrida, Phys. Rep. 301 (1998) 65.
[2] G.M. Schütz, in: C. Domb, J.L. Lebowitz (Eds.), Phase Transitions and Critical Phenomena, vol. 19, Academic Press, San Diego, 2001.
[3] J.T. MacDonald, J.H. Gibbs, A.C. Pipkin, Biopolymers 6 (1968) 1.
[4] G.M. Schütz, Europhys. Lett. 48 (1999) 623.
[5] T. Chou, Phys. Rev. Lett. 80 (1998) 85.
[6] B. Widom, J.L. Viovy, A.D. Defontaines, J. Phys. I 1 (1991) 1759.
[7] S. Klumpp, R. Lipowsky, J. Stat. Phys. 113 (2003) 233.
[8] L.B. Shaw, R.K.P. Zia, K.H. Lee, Phys. Rev. E 68 (2003) 021910.
[9] D. Chowdhury, L. Santen, A. Schadschneider, Phys. Rep. 329 (2000) 199.
[10] D. Helbing, Rev. Mod. Phys. 73 (2001) 1067.
[11] A. Schadschneider, Eur. Phys. J. B 10 (1999) 573.
[12] G. Schütz, E. Domany, J. Stat. Phys. 72 (1993) 277.
[13] M.R. Evans, N. Rajewsky, E.R. Speer, J. Stat. Phys. 95 (1999) 45.
[14] J. de Gier, B. Nienhuis, Phys. Rev. E 59 (1999) 4899.
[15] N. Rajewsky, L. Santen, A. Schadschneider, M. Schreckenberg, J. Stat. Phys. 92 (1998) 151.
[16] V. Popkov, I. Peschel, Phys. Rev. E 64 (2001) 026126.
[17] V. Popkov, G.M. Schütz, J. Stat. Phys. 112 (2003) 523.
[18] V. Popkov, J. Phys. A 37 (2004) 1545.
[19] E. Pronina, A.B. Kolomeisky, J. Phys. A 37 (2004) 9907.
[20] T. Mitsudo, H. Hayakawa, J. Phys. A 38 (2005) 3087.
[21] A. Parmegianni, T. Franosh, E. Frey, Phys. Rev. Lett. 90 (2003) 086601;
A. Parmegianni, T. Franosh, E. Frey, Phys. Rev. E 70 (2004) 046101.
[22] V. Popkov, et al., Phys. Rev. E 67 (2003) 066117.
[23] M.R. Evans, R. Juhász, L. Santen, Phys. Rev. E 68 (2003) 026117.
[24] E. Levine, R.D. Willmann, J. Phys. A 37 (2004) 3333.
[25] R. Juhász, L. Santen, J. Phys. A 37 (2004) 3933.
[26] I.T. Georgiev, B. Schmittmann, R.K.P. Zia, Phys. Rev. Lett. 94 (2005) 115701.
[27] The simulations show that the results remain essentially the same if lane changing is allowed on this site. This is because the densities on sites of (1,1) and (2,1) are same, therefore, the lane changing behaviors will not affect the densities on the two sites.
[28] Similarly, the results remains essentially the same if lane changing is allowed on this site.
[29] Note that in lane 1, the density at location $x<0.2$ essentially remains unchanged when Ω is small.
[30] Here the positions of the shocks are determined from mean-field predictions because the shocks have finite width and their positions are difficult to identify in finite system.
[31] The term $\langle\tau_{1,i}\tau_{1,i+1}(1-\tau_{2,i})\rangle$ is replaced by $\rho_{1,i}\rho_{1,i+1}(1-\rho_{2,i})$, and $\rho_{1,i+1}$ is approximated as $\rho_{1,i}$; similarly, the term $\langle\tau_{2,i}\tau_{2,i+1}(1-\tau_{1,i})\rangle$ is replaced by $\rho_{2,i}\rho_{2,i+1}(1-\rho_{1,i})$, and $\rho_{2,i+1}$ is approximated as $\rho_{2,i}$.